◆ Human Brain Mapping 3:257–270(1995) ◆

RESEARCH

Cortical Surface Modeling Reveals Gross Morphometric Correlates of Individual Differences

William C. Loftus, Mark Jude Tramo, and Michael S. Gazzaniga

Center for Neuroscience, University of California, Davis, California 95616 (W.C.L., M.S.G.), and Department of Neurobiology, Harvard Medical School and Neurology Service, Massachusetts General Hospital, Boston, Massachusetts 02115 (M.J.T.)

Abstract: Advances in human neurobiology are now made possible through methods which combine structural magnetic resonance imaging (MRI), three-dimensional reconstruction, and statistical analysis. MRI-based reconstruction enables the in vivo quantification of regional cortical surface area (rCSA) while inter-group comparisons uncover relationships of cortical morphometry with genotype, sex, and developmental abnormalities. In studies on normals we have found strong associations between the rCSA of monozygotic twins as compared to unrelated pairings. Further analysis of this data uncovered significant differences between the male and female twins in left hemisphere rCSA. When these methods were applied to brains of dyslexic subjects and controls, we identified a pattern of differences involving all major subdivisions of both hemispheres. Taken together, these techniques can illuminate structure–function issues in both normal and diseased brains. © 1996 Wiley-Liss, Inc.

Key words: cerebral cortex, cerebral hemispheres, telencephalon, magnetic resonance imaging, quantitative neuroanatomy, monozygotic twins, sex differences, dyslexia

INTRODUCTION

The modern technology for imaging brain structure and function now finds those studying neurobiologic issues in humans with powerful tools. In the explosion of activity over recent years, methodologies such as PET and fMRI have been developed and applied to measurements of metabolism and blood flow in anatomically and functionally differentiated parts of the brain, including the cerebral cortex. Other powerful techniques (e.g., ERPs, MEG) have been developed to measure the electrophysiological properties of the cerebral cortex. Perhaps the most straightforward area in human brain imaging research is the application of structural MRI and computer modeling to quantitative studies of gross neuroanatomy [Courchesne et al., 1994a; Damasio and Frank, 1992; Falk et al., 1991; Filipek et al., 1989; Kulynych et al., 1994; Myslobodsky et al., 1991; Rademacher et al., 1993b; Steinmetz et al., 1995; Suddath et al., 1990]. MRI provides direct measures of the static structural brain—not indirect measures of the dynamic functioning brain. In the following, our recent anatomical work is reviewed to illustrate how MRI combined with computer modeling techniques can be used to explore gross morphometric correlates of normal and abnormal brain function. Before turning to the methods employed in our studies, we begin with a brief survey of earlier methods of modeling and quantifying the cortical surface.

Cortical surface area measurement: rationale and techniques

The cerebral cortex has often been measured in terms of its total and regional volume [see for example Arndt et al., 1994; Filipek et al., 1989; Rademacher et al., 1993b]. Although cortical tissue occupies a volume, the cortex may also be viewed as an infinitely thin sheet having a surface area rather than a volume. Measures of cortical surface area (CSA) ignore the thickness through the laminae and reflect the *extent* of tissue rather than the sheer amount of it. The rationale for this, from an architectural standpoint, is that CSA is a macroscopic gauge of the number of processing units which are arranged perpendicularly to the surface. This view is supported by the observation that while the number of neurons in a given volume of cortex varies across cytoarchitectonic areas, the total number of neurons underlying a given unit of surface area is remarkably constant from one area to another (though striate cortex is an exception) [Rockel et al., 1980]. The imperfect correspondence of cytoarchitectonic boundaries with gyral and sulcal morphology complicates the interpretation of measures of regional cortical surface area (rCSA), as opposed to whole brain or total hemisphere measures. Nevertheless, the boundaries of primary architectonic fields bear some consistency to gross morphological landmarks [Rademacher et al., 1993a], and the primary determinants of gyrogenesis appear to be factors that are intrinsic, rather than extrinsic, to the cortex [Welker, 1990]. Compared to methods of estimating volume, there has been much variability among published methods of measuring CSA. Below, we review the advantages and pitfalls of the various techniques used specifically for the measurement of CSA.

Projection methods

Quantitative measures of rCSA have been performed on gross specimens, brain sections, and tomographic images [for review of early techniques, see Blinkov and Glezer, 1968]. An early technique was to apply a foil to the superficially exposed surface of the cortex of surface and to then measure the area of the foil. However, this could not be applied to the sulcal walls and fundi and was not widely used. The modern era in surface measurement is marked by the work of Geschwind and Levitsky [1968], who used photographs of the supratemporal plane to investigate possible left–right anatomical asymmetry of the posterior language region. Strictly speaking, this was not a surface area study since linear distances along the lateral margin of the planum temporale (PT) were measured. However, the photographs used in this study were later reexamined [Galaburda et al., 1987] by measuring the area of the PT with a planimeter. [For review of morphometric studies of asymmetry, see Witelson, 1977; and Witelson and Kigar, 1988.] Other authors [Rubens, 1977; Teszner et al., 1972; Witelson and Kigar, 1992] have also adopted photographic planimetry for the purposes of estimating CSA and lengths of fissures. This technique has the disadvantage that CSA estimates vary depending on how the specimen is oriented with respect to the image plane. Regions that are oriented obliquely are underestimated due to their foreshortened appearance in the image. Even if the camera orientation is precisely controlled, the planimetric area measures are still confounded with the local curvature of the surface. This issue has important implications for investigations of anatomical asymmetry, for it seems that the foreshortening of the left and right homologues cannot be equalized if they are folded differently [Loftus et al., 1993]. Such folding differences are common in the PT which is more likely to be bent on the right than on the left [Ono et al., 1991; Rubens et al., 1976; Steinmetz and Galaburda, 1991; Steinmetz et al., 1990c; Witelson and Kigar, 1992]. This confound can be mitigated by applying the procedure in a piecewise fashion to relatively planar subparts of structures. But this makes the procedure laborious, and has not been widely adopted.

A widely adopted technique which is more generally applicable than photographic planimetry involves the use of brain sections. The procedure, which may be applied to histological sections or MR images, is to: 1) trace the contours of structures on each slice, 2) estimate the surface area within each slice from the perimeter of the contours and spacing (or thickness) of the slices, and 3) integrate over the per slice estimates. This has an obvious advantage over photographic planimetry in that it takes account of the folding of the surface within each slice. However, a foreshortening artifact is still present in this method, because it fails to take into account the folding of the surface between sections. Unfortunately the error is not the same in all regions but varies with the slant of the cortical surface relative to the plane of the slice. Furthermore, it is not possible to compensate for it by increasing the density of slices. These estimates may be corrected by inflating them as a function of the discrepancy between successive contours, but this can be extremely laborious for highly convoluted structures, wherein the tilt between sections may fluctuate from region to region.

[For a discussion of correction methods for cross sectional techniques, see Blinkov and Glezer, 1968.]

Surface modeling vs. volume rendering

In the last several years, a wide range of graphic reconstruction techniques have emerged which produce three-dimensional images of the cortical surface from MR images. [For a comparison of different techniques, see Tiede et al., 1990; for an overview see Watt and Watt, 1992.] But not all of these techniques are appropriate for quantifying CSA. In this regard, it is important to distinguish between two broad classes of algorithms: *surface modeling* and *volume rendering.* Both of these operate on grey level volumes to produce graphic images of the cortex, yet one is superior to the other in terms of providing a geometrically sound foundation for surface area measurement.

This is the surface modeling approach wherein the grey level volume is not displayed directly but is used to first construct a polyhedral model, or "tessellation." This intermediate step of reconstructing the model by fitting polygons (usually triangles) to the grey level data can be accomplished in a variety of ways. The classic version of this approach is to first draw contours of the structure boundary as it appears on successive slices. This is followed by interpolating a sheet of polygons between consecutive contours. The actual algorithms for interpolating the surface can vary [Carman, 1990; Fuchs et al., 1977; Loftus et al., 1993; Schwartz et al., 1988; Winslow et al., 1987]. In another approach to surface modeling, the contour step is omitted and polygons are fitted directly into the data volume [Dale and Sereno, 1993; Lorensen and Cline, 1987]. In the latter method, the spatial continuity of the polygons emerges naturally from the coherence of the grey levels in the image volume. Both methods produce a piecewise planar sheet whose overall shape approximates the structure of interest. In a graphics context, this representation is input to a renderer which projects it to a viewing plane, and performs hidden surface removal and polygon shading. From a quantitative perspective, the model is an end in its own right, and its surface area can be precisely measured. The rendering may be useful insofar as it can assist an operator in subdividing the model for regional measurements [Loftus et al., 1995].

Implicit in the surface modeling approach is the idea of *segmentation,* or classification of voxels into different structures according to the grey levels. The edge of cortex on the exposed gyral crowns can be easily segmented from the adjacent cerebral spinal fluid (CSF). However, surfaces of the opposing walls of sulci pose a problem for segmentation in that the edge information tends to be obscured in the tightly packed "potential spaces." While a human operator can easily identify the infolded surface of cortex, algorithms which rely on automatic identification of the cortical surface perform less reliably. Recently, this has been approached by constructing models of the deeper layers of cortex [Dale and Sereno, 1993]. This is easily accomplished since the border of the cortex with the white matter is more apparent. The model can then be gradually deformed to lie closer to the pial surface.

In the volume rendering approach [Levoy, 1988] the step of building the model is omitted and the volume of data is displayed in a more direct fashion. The basic idea is to project rays from a viewpoint back into the data volume. The attributes (e.g., grey levels, depth, opacity) of successive voxels lying along these rays are combined and mapped to a grey level which is then projected to the image plane. The application of volume rendering to quantifying CSA involves measuring the area (in pixels) subtended by the displayed image of a structure. Different facets of the structure are measured by rotating them into view. Inlying portions of the structure can be revealed by digitally "dissecting" away overlying portions [Kulynych et al., 1994]. It is important to realize that despite the apparent "3D" quality of these images, the measurement technique is equivalent to photographic planimetry and is therefore prone to the same limitations and distortions discussed earlier. The inherent flaw is that it hinges on the *appearance* of the object from some point of view instead of its intrinsic three dimensional coordinates. From a graphics perspective, the volume rendering approach has some advantages. It maps naturally onto domains where it is not possible to segment voxels due to "fuzziness" of structure boundaries, when an effect of translucency is needed [Tiede et al., 1990], or when rendering brain lesions [Damasio and Frank, 1992]. However, for the purposes of surface area measurement, the surface modeling approach is superior.

Surface flattening

The primary motivation for computationally flattening the cortex has been to simplify the spatial relationships of cortical areas [Van Essen and Maunsell, 1980], or as way to map architectural [Schwartz et al., 1989] or functional data [Carman, 1990] in two dimensions. It might also seem that flattening the cortex may simplify CSA measurements, but this position is largely fallacious. Early approaches to flattening contours are

drawn of each section. The contours are "unraveled," while preserving their lengths, and placed side by side in the plane. In one variant, the contours are completely straightened and placed a constant distance apart [e.g., Falzi et al., 1982; Jouandet et al., 1989; Larsen et al., 1989]. The distance is determined by the slice width or separation. The CSA is estimated from the area of the resulting planar map. Quantitatively, this procedure is equivalent to the cross sectional contour method critiqued earlier and is therefore prone to foreshortening distortion. In a more general technique, the contours are partially unraveled which allows the distance between consecutive contours to be modulated so as to compensate for the surface tilt between sections [Van Essen and Maunsell, 1980]. The modulation of intercontour distances is analogous to the laborious corrections described earlier for the cross section method. Ironically, the basic weakness in this type of flattening stems from the lack of a 3D model to begin with.

There have been more rigorous efforts to computationally flatten a 3D polyhedral model of visual cortex [Carman, 1990; Schwartz et al., 1989]. Typically, some measure of distortion is computed locally at each vertex. As the model is deformed to the plane, numerical techniques are used to find configurations of vertices that globally minimize the distortion in surface area (usually at the expense of introducing distortions in connectivity or angular relationships). However, as already implied, the flattening operation is superfluous with respect to estimating CSA, which can be readily obtained from the (undeformed) polyhedral model. With a few exceptions, it is difficult to rationalize the use of computational flattening for quantitation, when any measure that is obtained from 2D map could just as easily be obtained from the 3D model. Cortical flattening may illuminate relationships that would not have been appreciated from viewing a folded 3D model, but it is a superfluous procedure from the perspective of CSA measurement.

METHODS: IMAGING AND RECONSTRUCTION

We now turn to the 3D reconstruction methodology we employed to obtain quantitative measures of the surface area of the entire cortex and morphological subdivisions.

Imaging

MR images were acquired in the coronal plane with either a Siemens 1.0 Magnetom system or a General Electric 1.5 Signa system. Acquisitions were T1-weighted to provide good grey/white contrast and spatial resolution (GE: TE/TR = 9 ms/50 ms; Siemens: 20/400 ms) Slice thickness was 3.0 mm with no interslice gap. All images were 256 × 256 pixels, with an interpixel distance of 0.937 mm (GE) or 1.2 mm (Siemens). The head was aligned in the magnet so that a horizontal laser marked the intercanthal line and a vertical laser intersected the midpoint of the nasion and philtrum. Alignment in the sagittal plane was checked by verifying the presence of midline structures on the same midsagittal locator image. Coronal sections were inspected to avoid obvious left-right asymmetries in the appearance of gyri, the frontal horns, the thalami, and cerebellar hemispheres.

Images were transferred to a Silicon Graphics workstation where models of both hemispheres in each subject were constructed and measured by a four-step procedure [Tramo et al., 1995]: 1) contours of the cortical ribbon on each section were hand traced with a cursor; 2) contour points were labeled according to the various gyri; 3) a triangular mesh surface was automatically interpolated between contours on consecutive slices; and 4) surface areas of triangles were computed automatically and attributed to a region based on the labels of the vertices. Each of these steps is elaborated below.

Cortical contours

The first two steps in this procedure were adapted from Jouandet et al. [1989]. The cortex was outlined directly on the workstation monitor. The MR image was magnified by a factor of three and a one-pixel wide contour was drawn with a cursor (Figs. 1 and 2). The outlining began on the medial surface, proceeded dorsally, laterally, and ventrally, and terminated medially. On slices where the corpus callosum was present, the contour started and ended at its dorsal and ventral surfaces. The contour was situated at the boundary between the grey matter and the CSF. Contiguous MR images were traced to yield about 55 contours per hemisphere. Inter- and intra-rater reliability of the cortical contour aspect of the procedure has been previously reported [Jouandet et al., 1990].

Delineation of *gyri*

The identification of the gyri in each image proceeded manually with the aid of hard copies which facilitated the scrutinization of several contiguous images at once. Structures were identified using the atlases of Krieg [1963], Matsui and Hirano [1978], and Talairach and Tournoux [1988]. Most of the regions of

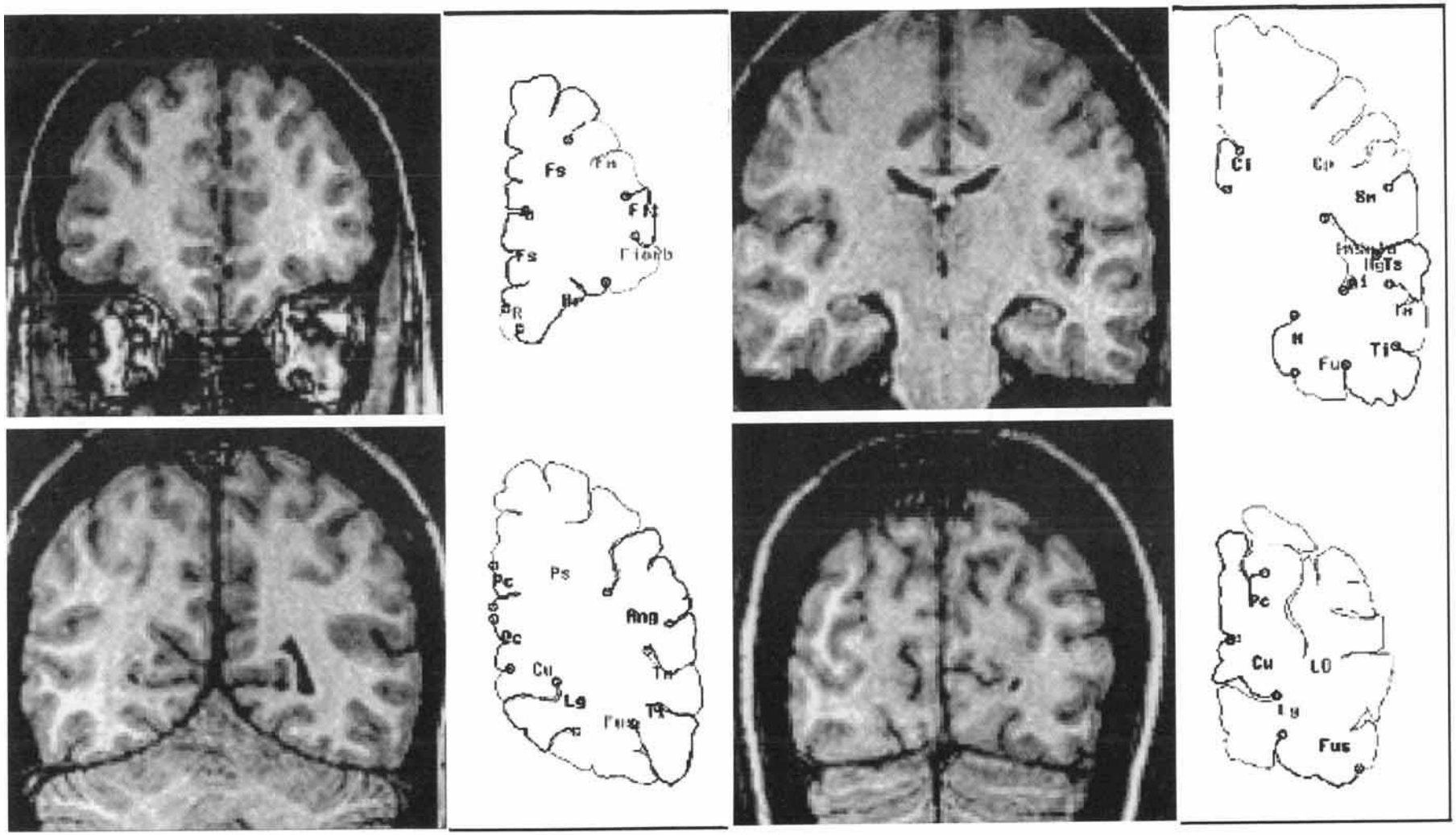

Figure 1.

Four of 60 coronal MR images of one subject. Corresponding outlines of the left hemisphere cortical surface appear to the right of each image. The images are arranged from anterior (**upper left**) to posterior (**lower right**). The contours extend into intrasulcal spaces as well as the superficially exposed gyral crowns. Circles at the fundi subdivide the contour into segments which are classified according to the region (see Table I).

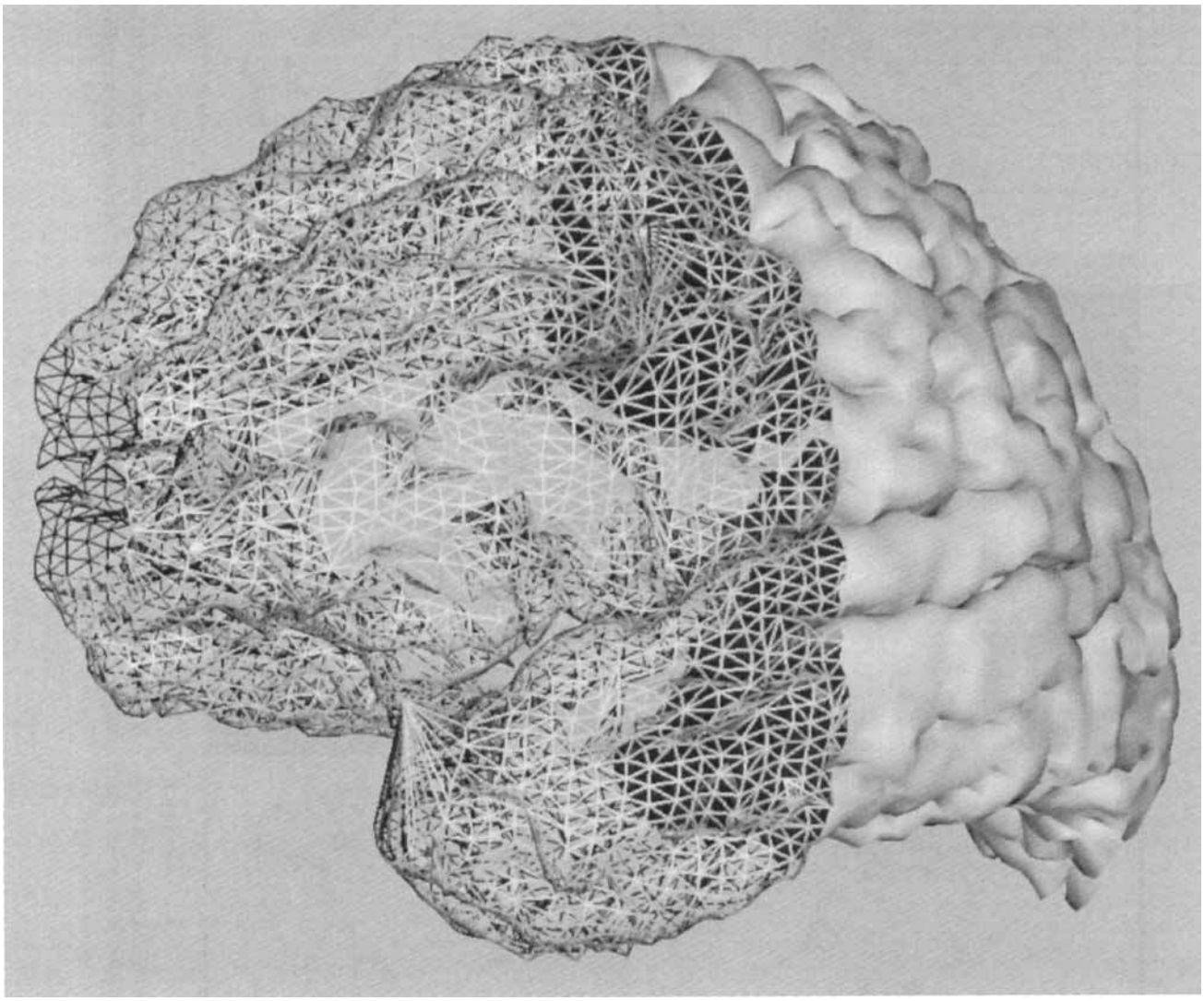

Figure 2.
A 3-D rendering of a surface model of one hemisphere. A triangle mesh is interpolated between consecutive contours to create the model. Regional surface area is computed by summing the area of the triangles in different portions of the model.

interest (ROIs) in the coronal MR images could be identified using atlas images on the basis of the relative position along the anteroposterior axis and the hemispheric quadrant of the ROI within each section. If the boundary between two gyri still could not be unambiguously localized, other features were used as cues. These features included: the relative locations of other identifiable gyri and sulci, the depth and orientation of surrounding sulci, and the branching pattern of gyri within and across serial sections. The frontal pole was identified as the surfaces anterior to the first section in which the superior and inferior frontal sulci were visible. The temporal pole was identified as the surfaces anterior to the first section in which the superior and inferior temporal gyri were visible. The occipital pole was identified as the surface posterior to the last section in which the occipital sulcus was visible. These assignments were notated on printouts of the contours before they were encoded. This was accomplished with a graphical interface which permitted the operator to subdivide contours by placing markers at the fundi of the sulci. The appropriate label from a pop-up menu was then assigned to segment of the contour lying between the markers. Figure 1 shows four contours after the completion of these steps. All the ROIs that

TABLE I. Regions of interest (ROIs)

Frontal lobe	Parietal lobe	Temporal lobe	Occipital lobe	Other
superior frontal g	postcentral g	superior temporal g	lateral occipital g	cingulate g
middle frontal g	supramarginal g	middle temporal g	cuneus	basal forebrain
pars orbitalis	angular g	inferior temporal g	lingual g	insula
pars triangularis	superior parietal lobule	transverse g	occipital pole	
pars opercularis	precuneus	parahippocampal g		
precentral g		amygdala		
orbitofrontal g		uncus		
straight g		fusiform g		
frontal pole		parainsular region		
		temporal isthmus		
		temporal pole		

were identified and measured are listed by lobe in Table I.

Surface interpolation

In this step, each pair of consecutive contours was automatically "stitched together" so that a smooth surface "skin" stretched between them. The entire surface was determined by repeating the interpolation for all pairs of contours (i.e., between contours 1 and 2, then between contours 2 and 3, etc.). Computing the segments of the surface could be reduced to connecting points on the two contours, so that the connecting lines formed a mesh of triangles. Since the same pair of contours could be connected with many different possible meshes, an objective procedure was needed to select the mesh. This was important because different meshes have different surface areas. Therefore, we used a dynamic programming procedure [Cormen et al., 1990; Fuchs et al., 1977] to compute the mesh with the smallest possible surface area. Thus, given the set of contours, the interpolation procedure covered the contours with the least amount of "skin" possible. Each model could also be visualized and rotated on the workstation monitor. As seen in Figure 2, the model is locally flat but globally curved. The curved features mould to the gyri and sulci while the smaller triangular tiles enable quantification.

Surface area computation

The surface area of each triangle in the model was automatically computed from the cross product of its edges [Fraleigh and Beauregard, 1987]. The surface area of the triangle was then attributed to one of the 32 regions, depending on the label information stored at the triangle vertices. Some triangles were "transitory," appearing near the boundary of different gyri so that the labels stored at each vertex of the same triangle were different. In these cases, the surface area was attributed to all of the abutting gyri. The rCSA of lobar subdivision was estimated from the rCSA of the component gyri (see Table I). The surface area of the entire hemisphere was obtained from the sum of all the triangles in the model.

APPLICATIONS

We now turn to some applications of the technique described above. Briefly, the basic questions addressed are as follows: 1) how *similar* is the surface area of monozygotic twins? Could it be the well-known correlations in twins with respect to cognitive and other behavioral measures might be reflected in brain measures? 2) How *different* are the sexes with respect to cerebral morphology in general? 3) What aberrations in the regional distribution of CSA are found in subjects diagnosed with developmental dyslexia?

Cortical morphometry in monozygotic twins

In a study which predated the development of our methods of measuring CSA, we examined the role genes play in brain development by looking for similarities that might exist in the size and shape of the corpus callosum in normal monozygotic twins [Oppenheim et al., 1989]. The callosum was visualized in five pairs of twins using the mid-sagittal alignment method described earlier. Callosal area correlated significantly within twin pairs but not within control pairs. In addition, the percent pixel overlap of the images from co-twins was significantly greater than the overlap of unrelated individuals. We recently reproduced these findings on another set of five twin pairs (Fig. 3). This

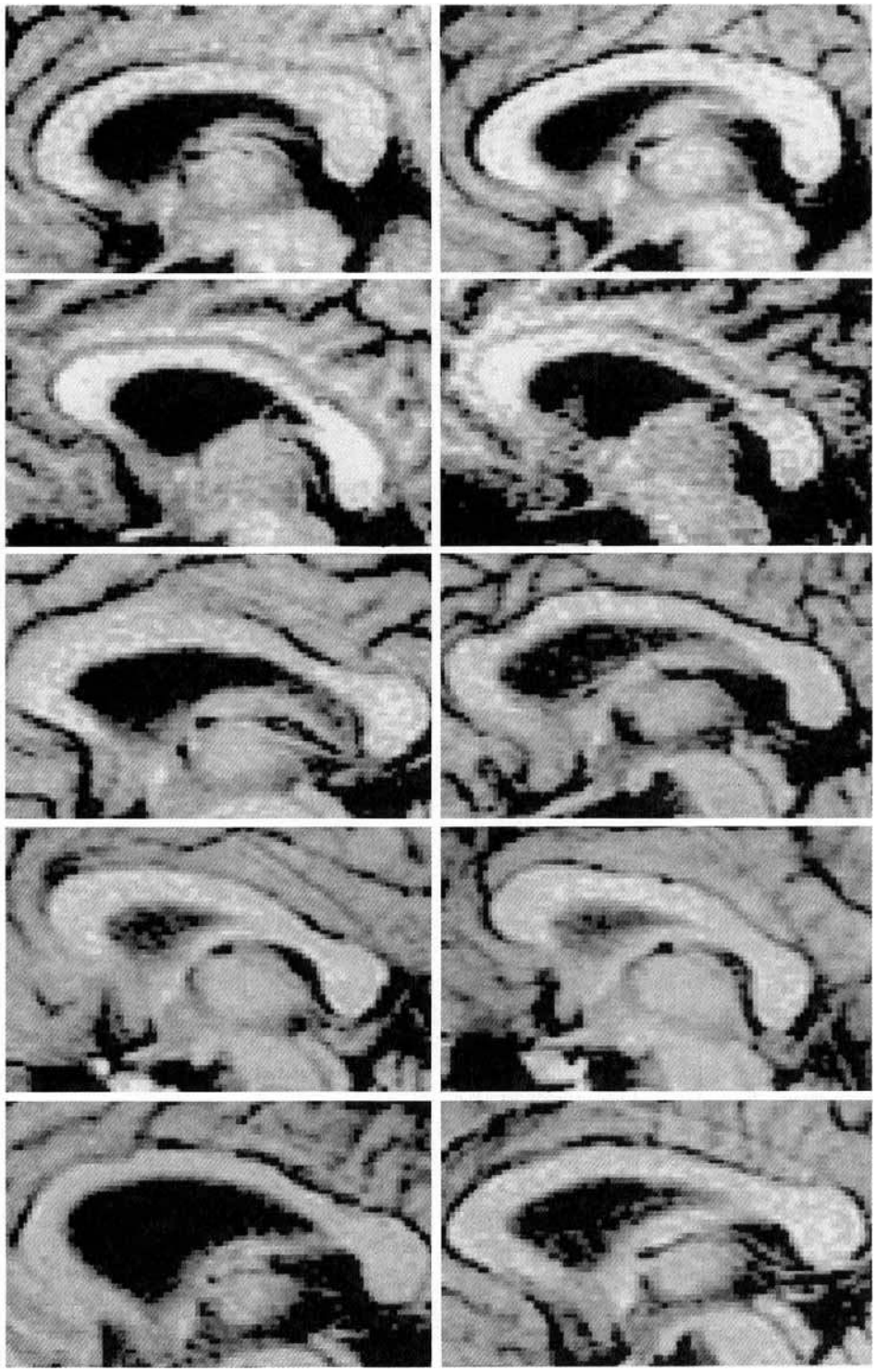

Figure 3.
Comparison of callosa of five pairs of identical twins. Similarities within twin pairs in the same row are seen relative to the differences among the different pairs.

TABLE II. Difference score ranks and probabilities of twin pairings vs. all other possible pairings

	Ten twin pairs (3,628,800 pairings)		Male twins (5 pairs, 120 pairings)		Female twins (5 pairs, 120 pairings)	
	Left hemisphere	Right hemisphere	Left hemisphere	Right hemisphere	Left hemisphere	Right hemisphere
Raw	99.999421	99.596	98.33	94.166	99.1666[a]	99.1666[a]
	<.000012	<.0081	<.0334	.117	.0168	.0168
Normalized	99.9529	96.2828	99.1666[a]	91.67	99.1666[a]	97.5
	<.001	<.08	.0168	.166	.0168	.05

[a] Rank is highest possible.

promising result encouraged us to analyze the entire cerebral cortex and its gross morphological subdivisions in twins [Tramo et al., 1995].

The rCSA of five pairs of female and five pairs of male monozygotic twins was measured. All subjects were right handed. Monozygosity was determined with red blood cell surface markers and by a standardized questionnaire [Cederlof et al., 1961; Lee and Lebeck, 1984]. Handedness was assessed by questionnaire [Oldfield, 1971]. In order to address the question of whether some association existed between brains of twin pairs, a difference measure was computed for each hemisphere in each pair of twins. That is, the absolute value of the difference in siblings' scores on each regional measure was computed. The resulting 32 differences, one for each region, were summed to give a difference score for a pair. Thus, a score of zero would indicate that the regional surface area of the twins was identical. As regional measures diverge between co-twins, the difference score takes on increasing values. Difference scores were calculated for 10 pairs of twins and summed to yield an overall score for the whole set twins, which is reported here.

The difference score does not by itself carry any indication of the association between twins' brains. To approach this question, some way of comparing the difference score to an appropriate control distribution is required. This distribution was computed from the same 10 pairs of twins by pairing up individuals regardless of whether or not they were related, and deriving overall difference score for these artificial pairings. Given an N of 10 twin pairs, there are 10! = 3,628,800 possible pairings. The difference scores associated with all of the pairings were computed and rank ordered. If the difference score for twins ranked low, it would suggest there was similarity involving regional surface area in co-twins. This is what was found. Using the percentile rank as an exact one-tailed probability, the results for both left and right hemisphere were highly significant (left, $P < .000006$; right, $P < .004$). In order to remove possible contributions of sex differences to these effects, separate analyses were performed for males and females. For the five pairs of females, the obtained error score of both hemispheres was the smallest of all the 5! = 120 scores ($P < .008$, both hemispheres). More modest effects were also present in the males (left, $P < 0.02$; right, $P < 0.06$). In order to separate regional effects from global size effects, the raw surface area data were normalized by total hemisphere surface area and the percentages were analyzed with the same technique. The same pattern of effects was maintained. Table II summarizes the results. The regional effects for both raw and normalized data have been confirmed with parametric statistical procedures, described elsewhere [Tramo et al., 1995], which compared the variance within co-twins to the variance across all the twin pairs. These results of these tests also showed less variation within co-twins than across unrelated pairs, even when the effects of birth order and sex on variance were taken into account. Thus we have now found twin similarities involving cortical surface area as well as callosal cross-sectional area. We interpret the results of our in vivo measurements as evidence of genetic factors influencing the size and shape of the human brain.

Sex differences

It is interesting that in the above analysis, the effect of monozygosity was more apparent in females than in males. In order to directly compare the sexes, an analysis of variance was performed with rCSA as the dependent variable and sex and ROI as factors. Separate analyses were carried out for each hemisphere. For the normalized rCSA measures, there was a significant interaction of sex and ROI in the left hemisphere ($P = 0.007$) but not in the right hemisphere ($P = 0.50$). Since regional (e.g., gyral) surface

area was normalized by total cortical surface area, it is unlikely that this sex difference arose from overall size differences between females and males. This sex effect disappeared when the data were analyzed in terms of lobar percentages, making it difficult to attribute a clear cut pattern to the sex effects. Moreover, there was no significant difference between the sexes in raw total CSA or total CSA normalized by body weight. But these results do suggest that the folding of the left cerebral cortex is quite different in females and males. The lack of a right hemisphere sex effect is not completely surprising, given that we obtained weaker genotype effects in the right hemisphere. To the extent that gross morphological measures reflect the organization of functionally specialized subsystems, we speculate that sex differences in left hemisphere organization are related to the morphometric differences. Based on lesion effects, it has been suggested [Kimura, 1983, 1987] that within the left hemisphere, brain organization for basic speech and praxis is organized more focally in women than in men. These apparent differences in organization may relate to differences in ability on standardized test performance in normals [Gleitman, 1981; Halpern, 1986; Harshman et al., 1983; Maccoby and Jacklion, 1974]; however, a meta-analysis suggests that the differences may be only slight [Hyde and Linn, 1988].

Cortical morphometry in dyslexia

As more digital data are banked, statistical analyses will become increasingly powerful. For now, it appears that the present approach is likely to yield interesting information about abnormalities afflicting this part of the central nervous system. The pattern of consequent behavioral disturbances may be correlated with the pattern of pathoanatomical findings. One such disturbance afflicting the cerebral cortex is congenital dyslexia. We measured regional cortical surface area in eight college-educated dyslexic volunteers and a control group matched for age, handedness, and educational level [Loftus et al., 1994]. All subjects were right handed males, aged 19–32 years, and had no history of other neurologic or psychiatric illness. Dyslexics were diagnosed by a learning disabilities specialist on the basis of standard neuropsychological and educational achievement tests. An analysis of variance showed a significant group (dyslexic vs. control) by cortical region interaction ($P < .0001$). This interaction was also found when analyses were performed separately for each hemisphere (left, $P < .0001$; right, $P = .0007$). No significant size difference was found for the hemispheres as a whole. Nevertheless, in order to eliminate the possibility that these effects were due to a global size difference, the data were normalized by whole hemisphere surface area in the same manner as in the cortical morphometry and sex differences studies. A similar pattern of results was obtained from the normalized data.

The nature of these differences is more apparent when the regional measures are summed to obtain lobar measures. Figure 4 compares the lobar data for both groups in terms of the raw and hemisphere normalized surface area. These data suggest that at least two types of trends are occurring in parallel: 1) dyslexics have a higher ratio of parietal to temporal CSA in both hemispheres, with a somewhat greater effect on the left; and 2) the pattern of left–right asymmetries is altered in dyslexia. Figure 5 (top) shows a significant difference between the groups ($P < .04$) in terms of the ratio of parietal/temporal surface area. Figure 5 (bottom) shows the normalized left/right differences for the frontal and occipital regions which show a significant interaction ($P < .006$) between group and lobe. These results suggest that neurodevelopmental disturbances underlying dyslexia are associated with widespread yet specific pathoanatomic changes that are detectable at the gross morphological level.

DISCUSSION

In these studies MRI was combined with three-dimensional surface modeling to measure rCSA in small subject populations. To our knowledge, this represents the first application of these technologies to obtain surface area measures of the entire cerebral cortex and its morphological subdivisions. Analyses of the hemispheric proportions of rCSA in different subject populations suggest there are: 1) genetic influences on the relative size of subregions, 2) sex-related differences in the distribution of rCSA within the left hemisphere, and 3) a trend toward an altered distribution of lobar surface area in both hemispheres in learning-disabled subjects.

Two related aspects of the current approach which distinguish it from earlier in vivo morphometric studies are the abilities to 1) take account of total CSA and 2) measure multiple regions. By normalizing the regional data by total hemispheric surface area, it was found, independent of stature or other global size variables, that individual differences may have a lot to do with the relative size of cortical structures as well as their absolute size. In the context of the dyslexic subject analysis, it suggests that there are local surface features that are altered. These alterations may reflect

imbalances among functionally specified regions within the cortex rather than the size of the structures per se. The characterization of CSA alterations was enhanced by considering the pattern of area differences across the entire cortical surface rather than focusing on a single region. The global effects found here make intuitive sense given the prevailing view

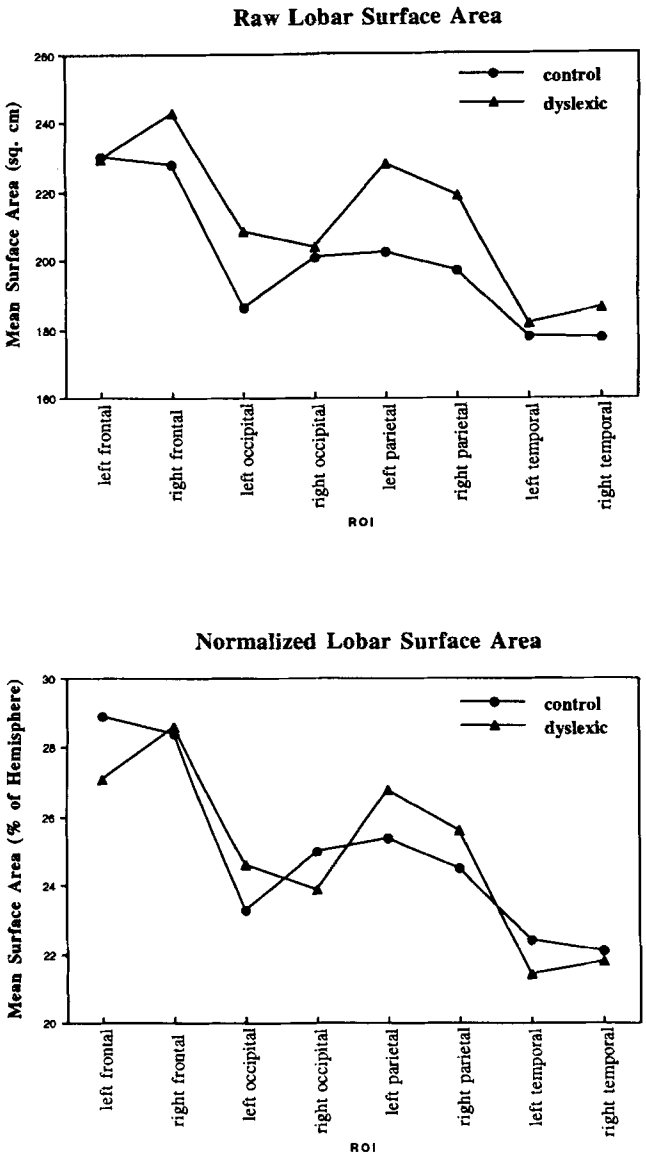

Figure 4.
Raw surface area (**top**) and percentage surface area (**bottom**) as a function of lobe. Raw surface area shows a trend ($P < .08$) for a group × ROI interaction. The trend towards greater surface area overall in the dyslexics was not significant ($P = .14$). Percentage surface area shows a trend ($P < .07$) for a group × ROI interaction.

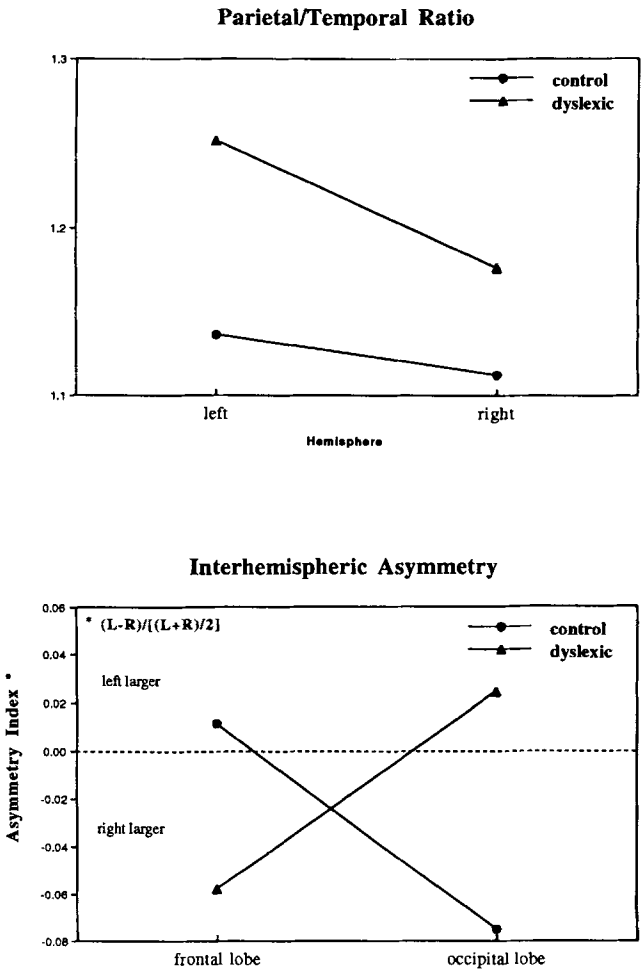

Figure 5.
Top: Parietal/Temporal ratio as a function of hemisphere. **Bottom:** Interhemispheric (left vs. right) asymmetry as a function of lobe (frontal/occipital).

that these syndromes involve multiple functionally specialized subsystems, some of which are distributed across a wide expanse of cortex. This complements previous work that pursued the question of anatomical disturbances in particular regions [for review see Duara et al., 1991; Galaburda, 1993; Hier et al., 1978; Leonard et al., 1993; Rumsey et al., 1986]. We suspect that this approach might also be fruitfully applied to morphometric investigations of schizophrenia, which have focused on frontal and temporal lobes [Andreasen et al., 1990; Buchsbaum, 1990; Crow et al., 1989; Crowe, 1990; Jernigan et al., 1991; Suddath et al., 1989, 1990]. The hypothesis that widespread changes in cortical organization are responsible for—or are concomitants of—disturbances such as dyslexia and schizophrenia is consistent with the evidence that

these disorders do not involve *unitary* defects in cognition but a *constellation* of circumscribed defects. The genetic influences on cortical morphometry uncovered in our twin studies may be the source of derangements observed in dyslexia and schizophrenia—disorders for which epidemiological evidence of a genetic cause exists.

From an anatomical standpoint, the thrust of this type of work runs counter to the prevailing approach in human brain mapping which minimizes structural variation by warping brains to a common template. This is motivated by the need to merge functional imaging data from different subjects [e.g., Evans et al., 1992; Fox et al., 1985]. Because structural variation is the focus of interest in our studies, it was deemed inappropriate to deform the MRI data to a standard template. Rather, each brain was labeled individually without reference to a standard coordinate system. We expect that the labeling of ROIs is a significant source of error due to the difficulty in precisely localizing the boundaries of gyri within and between sections. However, it is not clear that a template approach to labeling would have mitigated this error. This is because the gyral boundaries of different brains will rarely match even after they have been "matched" in terms of coordinate system [Steinmetz et al., 1989, 1990a, 1990b]. Thus, if the brains in our study were warped with fit to a stereotactic atlas, decisions regarding the placement of region boundaries would be made with reference to local surface topography, and not on the basis of standardized spatial coordinates. Other sources of error which may have reduced the sensitivity of the method are the inter-subject variability in angle of the coronal sections and the operator error in tracing the cortical contours. Although variance in slice angle may have severe confounding effects in 2D studies where analysis is restricted to single slices [Courchesne et al., 1994b] we believe it is less critical in the present context where the entire 3D volume is reconstructed. Though we acknowledge that these factors influence CSA measures, we believe that they did not vary systematically among subjects and therefore cannot account for the observed effects.

Conversely, the noise in rCSA measures may have prevented detection of group differences. Twin and sex effects in the right hemisphere which were weak may have reached statistical significance with more experimental precision. In the dyslexia study, there was also substantial overlap in the two distributions, notwithstanding the statistical differences in the mean lobe measures. An improved signal to noise ratio may have uncovered more distinctive differences between groups. There are existing software methodologies which promise to mitigate experimental error in CSA measurement. Accuracy in labeling may benefit by the capability to project points on slices onto surface reconstructions and other planes of section [e.g., Damasio and Frank, 1992; Steinmetz and Huang, 1991]. Reliability in surface modeling may be improved with algorithms which require less operator intervention in the segmenting of the cortex from the white matter and CSF [Dale and Sereno, 1993; Lorensen and Cline, 1987]. We are currently integrating these capabilities into a common interface for measuring gross morphological subdivisions [Loftus et al., 1995].

ACKNOWLEDGMENTS

Aided by ONR N00014-89-J-3035, NIH/NINDS P01 NS17778-10, the McDonnell-Pew Foundation, and NIH/NIDCD K08 DC00071.

REFERENCES

Andreasen NC, Ehrhardt JC, Swayze VW, Alliger RJ, Yuh WTC, Cohen G, Ziebell S (1990): Magnetic resonance imaging of the brain in schizophrenia. Arch Gen Psychiatry 47:35–44.

Arndt S, Swayze V, Cizadlo T, O'Leary D, Cohen G, Yuh WTC, Ehrhardt JC, Andreasen NC (1994): Evaluating and validating two methods for estimating brain structure volumes: Tessellation and simple pixel counting. NeuroImage 1:191–198.

Blinkov SM, Glezer II (1968): The human brain in figures and tables. A quantitative handbook. New York: Basic Books.

Buchsbaum MS (1990): Frontal lobes, basal ganglia, temporal lobes—three sites for schizophrenia? Schizophr Bull 16:377–378.

Carman GJ (1990): Mappings of the Cerebral Cortex. Pasadena: California Institute of Technology.

Cederlof R, Friberg L, Johnson E, Kaij L (1961): Studies on similarity diagnosis in twins with aid of mailed questionnaires. Acta Genet Med Gemellol (Roma) 11:338–362.

Cormen TH, Leiserson CE, Rivest RL (1990): Introduction to Algorithms. Cambridge, MA: MIT Press.

Courchesne E, Townsend J, Saitoh O (1994a): The brain in infantile autism: Posterior fossa structures are abnormal. Neurology 44:214–223.

Courchesne E, Yeung-Courchesne R, Egaas B (1994b): Methodology in neuroanatomic measurement. Neurology 44:203–208.

Crow TJ, Ball J, Bloom SR, Brown R, Bruton CJ, Colter N, Frith CD, Johnstone EC, Owens DGC, Roberts GW (1989): Schizophrenia as an anomaly of development of cerebral asymmetry. Arch Gen Psychiatry 46:1145–1150.

Crowe TJ (1990): Temporal lobe asymmetries as the key to the etiology of schizophrenia. Schizophr Bull 16:433–443.

Dale AM, Sereno MI (1993): Improved localization of cortical activity by combining EEG and MEG with MRI cortical surface reconstruction: A linear approach. J Cogn Neurosci 5:162–176.

Damasio H, Frank R (1992): Three-dimensional in vivo mapping of brain lesions in humans. Arch Neurol 49:137–143.

Duara R, Kushch A, Gross-Glenn K, Barker W, Jallad B, Pascal S, Loewenstein DA, Sheldon J, Rabin M, Levin B, Lubs H (1991): Neuroanatomic differences between dyslexic and normal readers on magnetic resonance imaging scans. Arch Neurol 48:410–416.

Evans AC, Marrett S, Neelin P, Collins L, Worsley K, Dai W, Milot S, Meyer E, Bub D (1992): Anatomical mapping of functional activation in stereotactic coordinate space. NeuroImage 1:43–53.

Falk D, Hildebolt C, Cheverud J, Kohn LA, Figiel G, Vannier M (1991): Human cortical asymmetries determined with 3D MR technology. J Neurosci Methods 39:185–191.

Falzi G, Perrone P, Vignolo LA (1982): Right-left asymmetry in anterior speech region. Arch Neurol 39:239–240.

Filipek PA, Kennedy DN, Caviness VS, Rossnick SL, Spraggins TA, Starewicz PM (1989): Magnetic resonance imaging-based brain morphometry: Development and application to normal subjects. Ann Neurol 25:61–67.

Fox PT, Perlmutter JS, Raichle ME (1985): A stereotactic method of anatomical localization for positron emission tomography. J Comput Assist Tomogr 9:141–153.

Fraleigh JB, Beauregard RA (1987): Linear Algebra. Reading, MA: Addison-Wesley.

Fuchs H, Kedem KD, Uselton SP (1977): Optimal surface reconstruction from planar contours. Commun ACM 20:693–702.

Galaburda AM (1993): Neurology of developmental dyslexia. Curr Opin Neurobiol 3:237–242.

Galaburda AM, Corsiglia J, Rosen GD, Sherman GF (1987): Planum temporale asymmetry, reappraisal since Geschwind and Levitsky. Neuropsychologia 25:853–868.

Geschwind N, Levitsky W (1968): Human brain: Left-right asymmetries in temporal speech region. Science 161:186–187.

Gleitman H (1981): Psychology. New York: Norton.

Halpern DF (1986): Sex Differences in Cognitive Abilities. Hillsdale, NJ: Erlbaum.

Harshman RA, Hampson W, Berenbaum SA (1983): Individual differences in cognitive abilities and brain organization, Part I: Sex and handedness differences in ability. Can J Psychol 37:144–192.

Hier DB, LeMay M, Rosenberger PB, Perlo VP (1978): Developmental dyslexia: Evidence for a subgroup with a reversal of cerebral asymmetry. Arch Neurol 35:90–92.

Hyde JS, Linn MC (1988): Gender differences in verbal ability: A meta-analysis. Psychol Bull 104:53–69.

Jernigan TL, Zisook S, Heaton RK, Moranville JT, Hesselink JR, Braff DL (1991): Magnetic resonance imaging abnormalities in lenticular nuclei and cerebral cortex in schizophrenia. Arch Gen Psychiatry 48:881–890.

Jouandet ML, Tramo MJ, Herron DM, Hermann A, Loftus WC, Bazell J, Gazzaniga MS (1989): Brainprints: Computer-generated two-dimensional maps of the human cerebral cortex in vivo. J Cogn Neurosci 1:88–117.

Jouandet ML, Tramo MJ, Thomas CE, Newton CH, Loftus WC, Weaver JB, Gazzaniga MS (1990): Brainprints: Inter- and intra-observer reliability. (abstract) Soc Neurosci Abstr 16:1151.

Kimura D (1983): Sex differences in cerebral organization for speech and practic functions. Can J Psychol 37:19–35.

Kimura D (1987): Are men's and women's brains really different? Can Psychol 28:133–147.

Krieg WJS (1963): Connections of the cerebral cortex. Evanston, IL: Brain Books.

Kulynych JJ, Vladar K, Jones DW, Weinberger DR (1994): Gender differences in the normal lateralization of the supratemporal cortex: MRI surface-rendering morphometry of Heschl's gyrus and the planum temporale. Cereb Cortex 4:107–118.

Larsen JP, Ødegaard H, Grude TH, Høien T (1989): Magnetic resonance imaging—a method of studying the size and asymmetry of the planum temporale. Acta Neurol Scand 80:438–443.

Lee CL, Lebeck LK (1984): Estimating dizygotic/monozygotic ratio of twins by general formula. Am J Clin Pathol 81:654–659.

Leonard CM, Voeller KK, Lombardino LJ, Morris MK, Hynd GW, Alexander AW, Andersen HG, Garofalakis M, Honeyman JC, Mao J, Agee OF, Staab EV (1993): Anomalous cerebral structure in dyslexia revealed with magnetic resonance imaging. Arch Neurol 50:461–469.

Levoy M (1988): Display of surfaces from volume data. IEEE Comput Graph Appl 8:29–37.

Loftus WC, Tramo MJ, Thomas CE, Green RL, Nordgren RA, Gazzaniga MS (1993): Three-dimensional quantitative analysis of hemispheric asymmetry in the human superior temporal region. Cereb Cortex 3:349–355.

Loftus WC, Green RL, Silberfarb A, Thomas CE, Nordgren RA, Nordgren RE, Gazzaniga MS (1994): Regional cortical surface area in subjects with developmental dyslexia. San Francisco, CA: Cognitive Neuroscience Society, p 85.

Loftus WC, Tramo MJ, Lutsep HL, Gazzaniga MS (1995): A three-dimensional technique for the reconstruction and measurement of human cerebral cortex and its gross morphological subdivisions in vivo. (abstract) Soc Neurosci Abstr 21:695.

Lorensen WE, Cline HE (1987): Marching cubes: A high resolution 3D surface construction algorithm. Comput Graph 21:163–169.

Maccoby EE, Jacklion CN (1974): The Psychology of Sex Differences. Stanford: Stanford University Press.

Matsui T, Hirano A (1978): An atlas of the human brain for computerized tomography. New York: Igaku-Shoin.

Myslobodsky MS, Glicksohn J, Coppola R, Weinberger DR (1991): Occipital lobe morphology in normal individuals assessed by magnetic resonance imaging (MRI). Vis Res 31:1677–1685.

Oldfield RC (1971): The assessment and analysis of handedness: The Edinburgh inventory. Neuropsychologia 9:97–113.

Ono M, Kubik S, Abernathey CD (1991): Atlas of the Cerebral Sulci. New York: Thieme.

Oppenheim JS, Skerry JE, Tramo MJ, Gazzaniga MS (1989): Magnetic resonance imaging morphology of the corpus callosum in monozygotic twins. Ann Neurol 26:100–104.

Rademacher J, Caviness VS, Steinmetz H, Galaburda AM (1993a): Topographical variation of the human primary cortices: Implications for neuroimaging, brain mapping, and neurobiology. Cereb Cortex 3:313–329.

Rademacher J, Galaburda AM, Kennedy DN, Filipek PA, Caviness VS (1993b): Human cerebral cortex: Localization, parcellation, and morphometry with magnetic resonance imaging. J Cogn Neurosci 4:352–374.

Rockel AJ, Hiorns RW, Powell TPS (1980): The basic uniformity in structure of neocortex. Brain 103:221–244.

Rubens AB (1977): Anatomical asymmetries of human cerebral cortex. In: Harnad S, Doty RW, Goldstein L, Jaynes J, Krauthamer G (eds): Lateralization in the Nervous System. New York: Academic, pp. 503–516.

Rubens AB, Mahowald MW, Hutton T (1976): Asymmetry of the lateral (sylvian) fissures in man. Neurology 26:620–624.

Rumsey JM, Dorwart R, Vermess M, Denckla MB, Kruesi MJP, Rapoport JL (1986): Magnetic resonance imaging of brain anatomy in severe developmental dyslexia. Arch Neurol 43:1045–1046.

Schwartz EL, Merker B, Wolfson E, Shaw A (1988): Applications of computer graphics and image processing to 2D and 3D modeling of the functional architecture of visual cortex. IEEE Comput Graph Appl 1988:13–23.

Schwartz EL, Shaw A, Wolfson E (1989): A numerical solution to the generalized mapmakers problem: Flattening non-convex polyhe-

dral surfaces. IEEE Trans Pattern Anal Mach Intell PAMI 11:1005–1008.

Steinmetz H, Galaburda AM (1991): Planum temporale asymmetry: In-vivo morphometry affords a new perspective for neurobehavioral research. Reading and Writing: An Interdisciplinary Journal 3:331–343.

Steinmetz H, Huang Y (1991): Two-dimensional mapping of brain surface anatomy. AJNR 12:997–1000.

Steinmetz H, Furst G, Freund HJ (1989): Cerebral cortical localization: Application and validation of the proportional grid system in MR imaging. J Comput Assist Tomogr 13:10–19.

Steinmetz H, Ebeling U, Huang YX, Kahn T (1990a): Sulcus topography of the parietal opercular region: an anatomic and MR study. Brain Lang 38:515–533.

Steinmetz H, Furst G, Freund HJ (1990b): Variation of perisylvian and calcarine anatomic landmarks within stereotaxic proportional coordinates. Am J Neuroradiol 11:1123–1130.

Steinmetz H, Rademacher J, Jancke L, Huang YX, Thron A, Zilles K (1990c): Total surface of temporoparietal intrasylvian cortex: Diverging left-right asymmetries. Brain Lang 39:357–372.

Steinmetz H, Herzog A, Schlaug G, Huang Y, Jäncke L (1995): Brain (a)symmetry in monozygotic twins. Cereb Cortex 5:296–300.

Suddath RL, Casanova MF, Goldberg TE, Daniel DG, Kelsoe JR, Weinberger DR (1989): Temporal lobe pathology in schizophrenia: A quantitative magnetic resonance imaging study. Am J Psychiatry 146:464–472.

Suddath RL, Christison GW, Torrey EF, Casanova MF, Weinberger DR (1990): Anatomical abnormalities in the brains of monozygotic twins discordant for schizophrenia. N Engl J Med 322:789–845.

Talairach J, Tournoux P (1988): Co-planar stereotaxic atlas of the human brain: A 3-dimensional proportional system, an approach to cerebral imaging. New York: Thieme.

Teszner D, Tzavaras A, Gruner J, Hécaen H (1972): L'asymetrie droite-gauche du planum temporale: A propos de l'etude anatomique de 100 cerveaux. Rev Neurol 126:444–449.

Tiede U, Hoehne KH, Bomans M, Pommert A, Riemer M, Wiebecke G (1990): Investigation of medical 3D-rendering algorithms. IEEE Comput Graph Appl 10:41–53.

Tramo MJ, Loftus WC, Thomas CE, Green RL, Mott LA, Gazzaniga MS (1995): Surface area of human cerebral cortex and its gross morphological subdivisions: In vivo measurements in monozygotic twins suggest differential hemisphere effects of genetic factors. J Cogn Neurosci 7:292–301.

Van Essen DC, Maunsell JHR (1980): Two-dimensional maps of the cerebral cortex. J Comp Neurol 191:255–281.

Watt A, Watt M (1992): Advanced Animation and Rendering Techniques: Theory and Practice. New York: ACM.

Welker W (1990): Why does cerebral cortex fissure and fold? A review of determinants of gyri and sulci. In: Jones EG, Peters A (eds): Comparative Structure and Evolution of Cerebral Cortex, Part II. New York: Plenum, pp. 3–136.

Winslow JL, Bjerknes M, Cheng H (1987): Three-dimensional reconstruction of biological objects using a graphics engine. Comput Biomed Res 20:583–602.

Witelson SF (1977): Anatomic asymmetry in the temporal lobes: Its documentation, phylogenesis, and relationship to functional asymmetry. Ann N Y Acad Sci 299:328–354.

Witelson SF, Kigar DL (1988): Asymmetry in brain function follows asymmetry in anatomical form: Gross, microscopic, postmortem and imaging studies. In: Boller F, Grafman J (eds): Handbook of Neuropsychology. New York: Elsevier, pp. 111–142.

Witelson SF, Kigar DL (1992): Sylvian fissure morphology and asymmetry in men and women: Bilateral differences in relation to handedness in men. J Comp Neurol 323:326–340.